KAERI/TR-1139/98

금속연료/HT-9 강의 공정반응 실험시방서

Experimental Specifications for Eutectic Reaction between Metallic Fuel and HT-9

October, 1998

한국원자력연구소

제출문

한국원자력연구소장 귀하

이 보고서를 "금속연료/HT-9강의 공정반응 실험시방서"의 기술보고서로 제출합니다.

1998. 10.

과제명 : 금속핵연료설계개발
주저자 : 황완
작성자 : 류우석, 남철, 이병운

책임감수위원 : 서인석
감 수 위 원 : 강영호

요약문

1. 목적 및 범위

연료와 피복관의 화학적 반응은 연료봉 설계에 있어서 중요한 고려사항이다. 고온에서 금속연료와 스테인레스 강 피복관이 접착하게 되면 다양한 원소의 복잡한 확산쌍(diffusion couple)이 형성되게 된다. 이렇게 형성된 확산영역은 두가지 중요한 문제점을 갖는다. 첫 번째는 피복관의 기계적 강도가 약해지는 점이고, 두 번째는 연료와 피복관의 경계면에서 융점이 낮아지는 공융현상이 나타난다.

이 두가지 영향을 평가하기 위해서, 확산쌍 실험을 계획하고 있다. 이 실험에서 사용될 확산쌍은 U-Zr 합금과 HT-9 스테인레스강이고, U-Zr 합금에는 8%, 10%, 12%의 Zr 농도가 사용된다. 이 실험의 주 목적은 HT-9 피복관을 가진 U-Zr 금속연료의 지르코늄 허용량을 평가하기 위한 실험 데이터를 생산하고, 이 결과를 문헌상의 10 wt% Zr 연료의 실험결과와 비교함으로써, 10 wt% Zr 의 기준치와 대등 또는 우세한 거동을 보이는 Zr 함량을 찾는데 있다. 또한 각 시편의 확산쌍 경계면에서 공융(eutetic) 현상이 일어나는 문턱 온도를 결정하고, 확산영역의 두께를 측정하기 위함이다. 본 보고서의 목적은 이러한 실험을 수행하기 위한 실험시방 항목에 대해 기술한다.

2. 실험 방법

U-Zr 합금을 제조하기 위해서는 depleted 우라늄을 사용한다. 3 가지 Zr 함량이 포함된 U-Zr 과 HT-9 의 확산쌍은 아르곤 분위기, 720～760℃의 온도범위에서 100～500 시간동안 소둔(annealing)한다. U-Zr 합금과 HT-9 피복재 디스크를 만들기 위해, 지름이 8mm 정도인 원통형 봉을 3mm 두께로 자른다. 잘라진 시편 조각은 SiC 종이위에 단면이 보이도록 내려놓고, 1μm diamond paste 로 polishing 한다. 이 과정은 시편 표면에 산화층을 없애기 위한 것이다. Polishing 하는 동안, 디스크의 두 면이 편편하고 각면이 서로 평행한지를 확인하기 위해, 두께를 측정한다.

ANL 의 실험은 확산쌍 실험에서 시편의 표면상태가 매우 중요함을 보여주고 있다. 시편의 표면이 깨끗하여 접촉상태가 좋으면 융점이 낮아지고, 반대로 표면에 이물질이 많으면 확산하는데 방해요소가 되어, 연료/피복관 경계면에서의 액상(liquid phase) 형성이 늦어지게 된다. 이는 불규칙한 접촉상태로 인해 일정한 공융온도 형성이 어렵기 때문이다.

Polishing 한 후, 즉시 연료, 피복관 시편을 '샌드위치'처럼 교대로, 3 개의 확산쌍이 형성되도록 fixture 에 쌓는다. 시편은 두 개의 end plate 로 구성된 지그(jig)

를 사용하여 고정한다. 이 fixture는 Kovar rod가 고정될 3개의 구멍(hole)이 있는 Kovar 합금(Fe-29Ni -17Co-0.3Mn-0.2Si, w/o) 디스크로 되어 있다. Kovar는 열 팽창 계수가 낮기 때문에 가열후 균일한 접촉면 형성에 유리하다. 시편을 쌓는 동안은 assembly의 brass pot-chuck을 잡고 있으면 된다. 시편 위에 위치한 Kovar 합금 디스크는 rod에 의해 중심을 맞춘다. 시편에 압축응력을 가하기 위해, 스테인레스강 너트(nut)를 rod에 조인다. 소둔하는 동안 Kovar 합금 봉과 시편의 열 팽창 차이는 시편의 축 방향 압축 load로 작용하게 된다.

U-Zr 합금 표면에 있는 산화막은 확산쌍에서의 확산을 방해하기 때문에, 시편준비, polishing, 확산쌍 어셈블리, 소둔, 분석 등의 모든 과정을 아르곤 분위기에서 행하거나, 특별한 polishing 처리로 산화막을 제거해야 한다. 한번 사용한 Kovar 지그를 재사용하려면 지그를 아르곤 분위기에서 노(furnace)에 넣고, 100시간동안 740~760℃에서 소둔한 다음, 아르곤 분위기에서 냉각한다.

시편의 산화를 줄이려면, fixture에 고정한 시편을 빨리 석영관에 넣어야 한다. 각 석영관에 아르곤을 몇번 흘려주고, 진공상태가 되게 한 다음, 밀봉하여 캡슐을 만든다. 가열속도는 약 10℃/sec로 하고 일정 온도에서 고정한다.

이 실험을 위해 선택된 온도 범위는 EM1~EM3 실험에 대해서는 U-Zr 합금/스테인레스강의 공융온도인 ~740℃가 포함된 740~760℃이고, EM4 실험에 대해서는 온도는 720℃이고, 유지시간은 500시간이다.

확산쌍을 소둔한 후, 캡슐은 공기중에서 냉각시킨다. 확산쌍을 석영 캡슐에서 꺼내고, 차가운 self-setting resin에 올려 놓는다. 그런 다음, 절단기를 사용하여 확산방향에 평행한 방향으로 단면이 드러나도록 시편을 세로로 자른다. 각 시편의 단면을 0.05μm 알루미나로 polishing 한다.

실험후, 시편은 공융현상과 연료와 HT9 간의 상호작용을 평가하기 위해 검사한다. 전체 확산조직에 걸친 상 구조(phase structure)를 확인하고, 성분원소의 분포도와 확산경로를 알기 위해, 광학 현미경, 분광기를 갖고 있는 SEM을 사용하여 시편을 분석한다.

피복재 길이의 기준값으로는 피복재의 가장 얇은 두께가 결정된다. 피복제의 실험전 두께와 실험후 두께는 피복재 침투 깊이로 정의될 수 있다.

3. 실험요건

3.1 균질화

연료합금은 900℃에서 4일 동안 균질화 시킨다. 그런 다음, EDX 또는 EPA(electron probe analyzer)를 사용한 조직검사를 수행한다.

3.2 산화

산화층을 제거하기 위해, 금속 연료와 HT9 봉의 표면은 0.1μm 알루미나로 polishing 한다. 소둔과 냉각 과정에는 시편의 산화를 막기위한 조치가 있어야 한다.

3.3 치수 측정

시편을 쌓기 전에, 각 시편의 두께는 ± 0.1mm 의 정확성을 갖고 측정한다. 각 시편의 두께는 서로 비슷해야 한다. 실험후에 반응층을 비교하기 위해서, HT9 시편 지름은 연료 시편 지름보다 커야 한다.

3.4 온도 조절

쌓여 있는 시편의 길이방향 온도 구배는 1℃보다 작아야 하고, 정상상태 (steady-state) 소둔 시 온도는 ± 4℃로 조절되어야 한다.

3.5 유지시간

실험의 유지시간을 결정하기 위해, 반응층의 최대 깊이는 금속 연료와 스테인레스 강 사이의 반응율의 상관식을 사용하여 실험 전에 평가하였다.

$$\dot{R} = \exp\left(11.646 - \frac{15665}{T}\right) \qquad (1)$$

여기서 R 은 반응속도(μm/sec)이며 T 는 온도(Kelvin)이다. 식 (1)은 1 시간 실험을 기준으로 만들어진 식이다.

800℃에서의 3 시간 동안의 실험으로 HT-9 시편의 2.2mm 의 반응층이 형성될 것으로 예상된다. 이것은 시편 조각의 두께가 5mm 일 때, HT9 의 44%가 손상되었음을 의미한다.

3.6 응력

실험하는 동안 반응층의 액화는 시편의 두께를 감소시키는 결과를 가져온다. 따라서 압축 응력은 소둔하는 동안 시편 집합체의 양쪽 면에 연속적으로 가해져야 한다.

4. 실험결과

확산실험 후, SEM, scanning Auger microscopy 분석 등을 통해 반응층의 미세구조적 변화를 관찰한다. 확산쌍에 대한 기술은 연료와 피복관의 상호 확산거동을

연구하기 위해 사용되었다. HT9 피복관의 확산거동을 U-10Zr 연료와 HT9 피복관의 연구를 통해 보고된 거동과 비교하기 위해, 비교 평가기준이 기술될 것이다.

다음은 설계값의 기준이 되는, 이 실험에 필요한 관련 실험결과를 기술한다.

4.1 문서와 실험결과

'금속핵연료설계개발'과제의 엔지니어가 사용승인하고, '금속연료제조기술개발'과제의 엔지니어가 준비하여 작성된 과정에 따라 실험을 수행한다. 모든 실험의 결과는 '금속핵연료설계개발'과제에서 발행되는 실험 보고서로 문서화 한다. 마지막 실험보고서는 revision 0 으로 발행된다.

4.2 비교 허용 기준

4.2.1 공융현상과 문턱 온도

광학 현미경은 시편에서 공융이 일어났는지를 결정하는데 사용된다. 공융을 보여주는 징후는 액상의 형성이다.

우라늄 연료에서 지르코늄의 양이 변하면 연료/피복관의 양립성과 합금의 녹는 온도가 변하게 된다. 만약 온도가 합금의 공융온도를 넘게 되면, 연료와 피복관과의 반응을 촉진시키는 액상과 고체상(solid phase)이 함께 형성된다.

실험하는 동안 관찰해야 하는 특성

- 액상의 광학적인 관찰
- 연료/피복관의 경계면에서 액상과 고체상의 혼합된 형태가 형성되는 각 합금의 문턱온도

4.2.2 피복재 침투와 피복재의 미세구조 변화

EMP(electron microprobe analysis)와 SEM 등을 사용하는 metallograpy 를 통해 액상현상의 증거를 찾고, 피복관과의 반응을 통한 침투 정도를 측정한다. 각 실험을 마친 후에, 보수적인 최대 침투값을 측정한다. FCI 의 기구(mechanism) 구명을 위해 EMP 와 SEM 를 이용하여 공융 후, 연료와 피복재에서의 상과 조성을 관찰한다.

- 총 6 번의 실험을 통해 얻은 피복관 최대 침투 깊이를 이전 데이터와 비교
- 실험온도에 따른 피복재 침투속도 변화
- 연료/피복재 사이의 확산층 분석

TABLE OF CONTENTS

Section **Title** **Page No.**

LIST OF TABLES

LIST OF FIGURES

1. SCOPE

Chemical interaction between fuel and cladding is one of the major concern in metallic fuel rod design. The contact of metallic fuel and stainless steel cladding in a fuel rod forms a complex multi-component diffusion couple at elevated temperatures. The potential problem of inter-diffusion of fuel and cladding components is essentially two-fold : weakening of cladding mechanical strength due to the formation of strength reducing diffusion zones in the cladding, and the formation of comparatively low melting point phases in the fuel/cladding interface to develop eutectic reaction.

In an attempt to assess the severity of these two deleterious effects prior to irradiation testing of specific fuel elements, diffusion couple experiments in the laboratory shall be customarily performed. Inter-diffusion of fuel and cladding components can in principle lead to several phenomena that could affect the reliable performance of a fuel rod.

In this experimental study, diffusion couples are consisted of U-Zr alloys and HT-9 material. Three diffusion couple experiments shall be conducted with U-Zr alloys which contain various zirconium contents from 8 % to 12% of Zr, such as, U-8%Zr, U-10%Zr, and U-12%Zr, to specifically assess the propensity for molten phase formation. This document gives the experimental specifications for the eutectic reaction experiment and chemical interaction between HT-9 cladding and various U-Zr fuels at the elevated temperatures. The experimental specifications cover the scope and purpose, design of test specimen, test set-up, test procedure, the requirements for the test, and test results and comparative acceptance criteria of eutectic reaction of U-(8-12 wt.%)Zr/HT9 test specimens.

2. PURPOSE

A key objective of this experiment is to produce experimental data to assess acceptable zirconium content for U-Zr alloy fuel with HT-9 cladding. According to the objective, the purposes of the eutectic reaction experiment between HT-9 cladding and U-Zr fuels with various contents of zirconium are as follows.

2.1 To investigate general thermal-design characteristics of U-Zr fuels with HT9 cladding, which the fuel slugs contain various zirconium contents from U-8%Zr, U-10%Zr, U-12%Zr.

2.2 To determine the threshold temperatures for eutectic formation at the interfaces of diffusion couples for each specimen.

2.3 To measure the diffusion zone widths(μm) of diffusion structures along with the types of phases that developed in the diffusion structures for each specimen of U-Zr/HT9 diffusion couples.

2.4 To compare the inter-diffusion behaviors in HT-9 cladding with the behaviors (Appendix B) reported in U-10Zr fuel versus HT-9 cladding steel investigations and to study the relative inter-diffusion behavior of the various fuels in the presence of different Zr weight and HT-9 cladding steel.

3. DESIGN CONCEPT OF TEST SPECIMEN

U-Zr fuels with various contents of zirconium up to 12 wt.% and HT-9 cladding samples shall be alternatively stacked, in columns of up to 3 samples as shown in Fig. 1. The test series consisted of four specimens, so called EM1, EM2, EM3, and EM4, alternatively stacked. Diffusion coupling specimens shall be equipped and installed according to the procedure and a guide described in chapter 4 and 6.

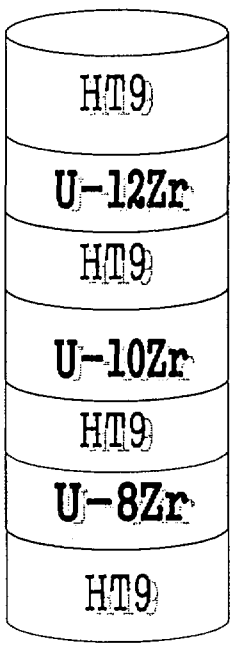

Fig. 1 Alternatively stacked specimen of diffusion couple test columns

4. TEST SET-UP

4.1 Diffusion couple and its assembly

Various U-Zr fuels and HT9 cladding samples shall be cut from cylinder bars to ~3 mm thick slices with approximately 8 mm in diameter. The binary alloys of U-Zr shall be prepared by 'metallic fuel fabrication technology development project', according to the internal guide and referring the design data of KALIMER fuel rod as shown in Appendix C. Depleted U shall be used in the preparation of the alloy using conventional induction melting methods. The HT-9 shall be provided by "metallic fuel design development project", which has nominal composition of HT-9 cladding as shown in Table 1.

The sample slices shall be ground flat on SiC paper to ensure parallel faces, and metallographically polished through 1 μm diamond paste. This procedure is employed to ensure that the surfaces shall be free from an oxide layer. Diffusion couples shall be assembled by stacking alternatively the fuel and cladding samples in columns of up to 3 samples. And they shall be placed in a Kovar alloy (Fe-29Ni-17Co-0.3Mn-0.2Si) jig that consisted of two Kovar end plates and three threaded Kovar rods. Kovar is a steel with a low coefficient of thermal expansion. Because oxide films on the surfaces of the U-Zr alloys prevent the diffusion process between the couples, all procedures including sample preparation, polishing, diffusion couple assembly, annealing, and analysis are performed in an argon atmosphere or the surfaces of the alloys are removed with a special polishing treatment.

To reuse the once assembled the Kovar jig, the jig shall be placed in a furnace under argon atmosphere and annealed at 740~760 ℃ for 100 hours and then quenched with argon.

U-Zr alloy system

The binary U-Zr phase diagram is presented in figure 2. There are three allotropes of solid uranium: orthorhombic U(α), tetragonal U(β) and body centered cubic (bcc) U(γ). The temperatures of transition are 942 K for U(α→β) and 1049 K for U(β→γ). Zirconium has two allotropes: close packed hexagonal (hcp) Zr(α) and bcc Zr(β). The transition temperature for Zr(α→β) is 1136 K. As shown in the diagram, solubility of Zr in U(α) or U(β) is very low. Similarly, solubility of U in

Zr(α) is very low. The two bcc phases, U(γ) and Zr(β), form a solid solution phase in which a miscibility gap exists. An intermediate phase (δ) is in a composition range of 67 – 73 at.% Zr, effectively UZr_2 with some solubility for Zr.

Fe-U and Cr-U alloy systems

The binary Fe-U phase diagram is presented in figure 3. There are two intermediate phases: U_6Fe at 14 at.% Fe and UFe_2 at 67 at.% Fe. In the diagram the most concerning point is a eutectic point at 725 ℃, 34 at.% Fe. Solubility of Fe in U is negligible. Solubility of U in Fe is also negligible.

The binary Cr-U phase diagram is presented in figure 4. There is not any intermediate phase. Solubility of Cr in U or U in Fe is very low. Only a eutectic point exists at 859 ℃, 20 at.% Cr.

Fe-Pu alloy system

The binary Fe-Pu phase diagram is presented in figure 5. Plutonium has six alloptropes: simple monoclinic Pu(α) (up to 122 ℃), body centered monoclinic Pu(β) (122 – 206 ℃), face centered orthorhombic Pu(γ) (206 – 319 ℃), fcc Pu(δ) (319 – 451 ℃), bct Pu(δ') (451 – 476 ℃), and bcc Pu(ε) (476 – 639 ℃). Of the six alloptropes, only delta phase plutonium is relatively stable or metastable. There are two intermetallic phases: Pu_6Fe and $PuFe_2$. A eutectic point at 10 at.% Fe shows low melting temperature at 410 ℃.

4.2 Annealing furnace and characterization

The assembled couples shall be placed in a quartz tube which is fabricated by "metallic fuel fabrication technology development project".

To reduce oxidation of the samples, the fixtured test column shall be quickly inserted into a quartz tube. Each quartz tube shall be flushed several times with argon, evacuated to vacuum, and sealed to form a capsule. The nominal test temperatures are 720 ℃ - 760 ℃ and are controlled within ±4 ℃. Annealing times of the majority of the tests are 100 hours with a few tests ending at 500 h, as shown in Table 2 and 3.

After annealing the couples, the capsules shall be allowed to cool in air. The diffused couples shall be removed from the quartz capsules and mounted in a cold self-setting resin. Mounted couples shall be then cut longitudinally using a cut-off

wheel to expose sections parallel to the direction of diffusion. The exposed cross section of each couple shall be metallographically polished through 0.05 μm alumina. The couples shall be analyzed using an optical microscope, scanning electron microscopy (SEM) with energy-dispersive spectroscopy to identify phase compositions throughout the diffusion structures and to generate composition profiles and diffusion paths. In turn, this information shall be used to calculate average effective inter-diffusion coefficients on both sides of the Matano plane, i.e., the plane of mass balance.

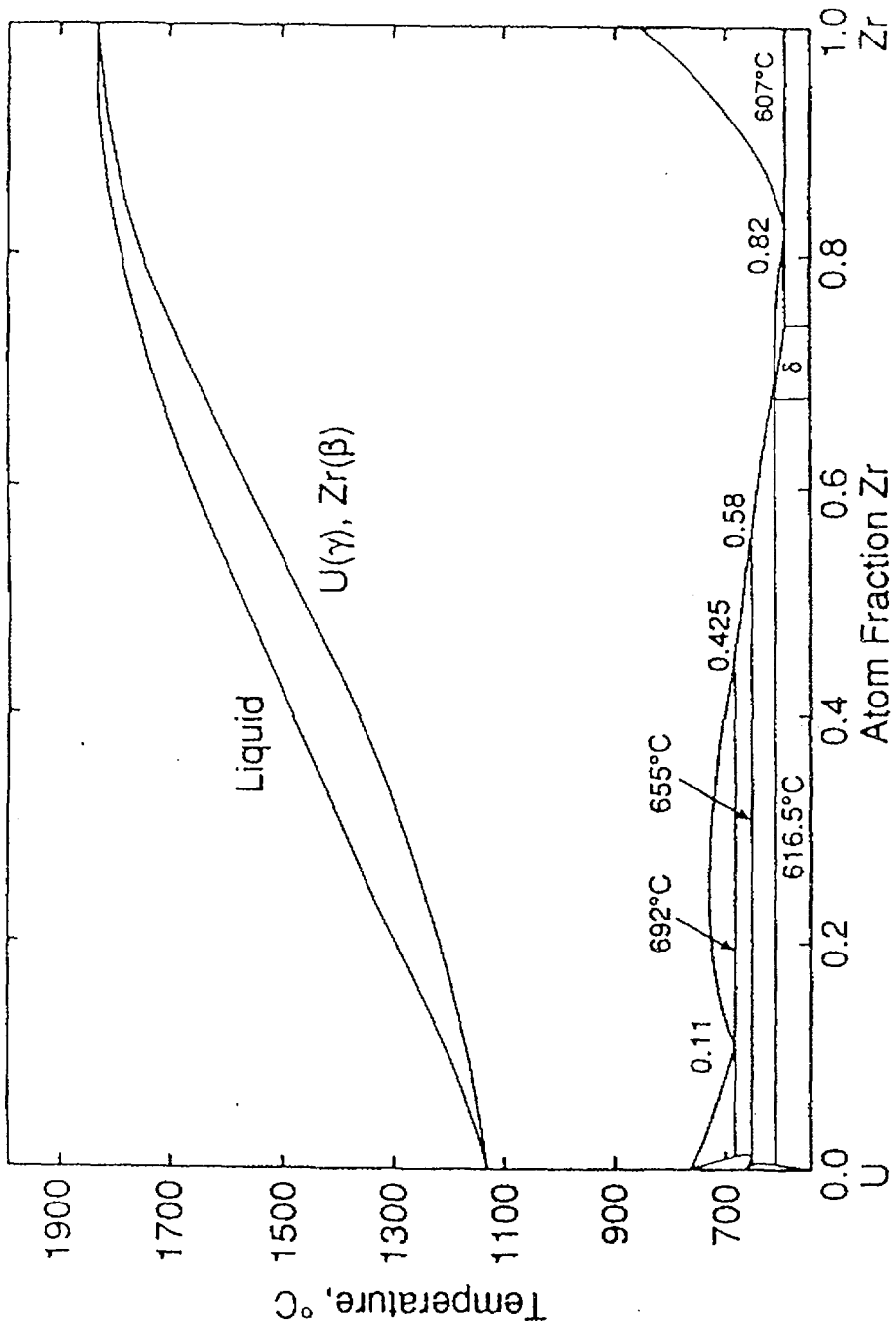

Figure 2. The binary U-Zr phase diagram

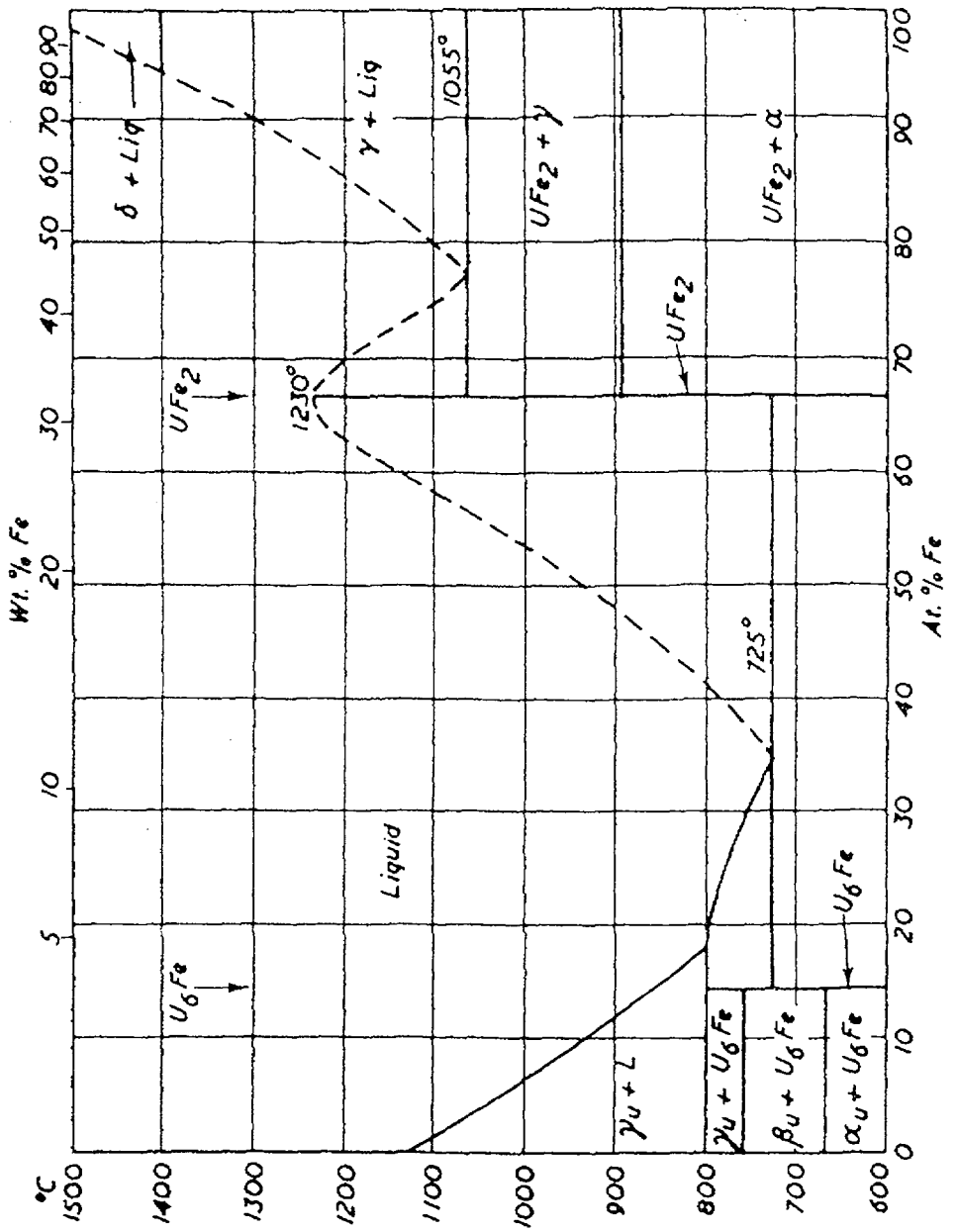

Figure 3. The binary Fe-U phase diagram

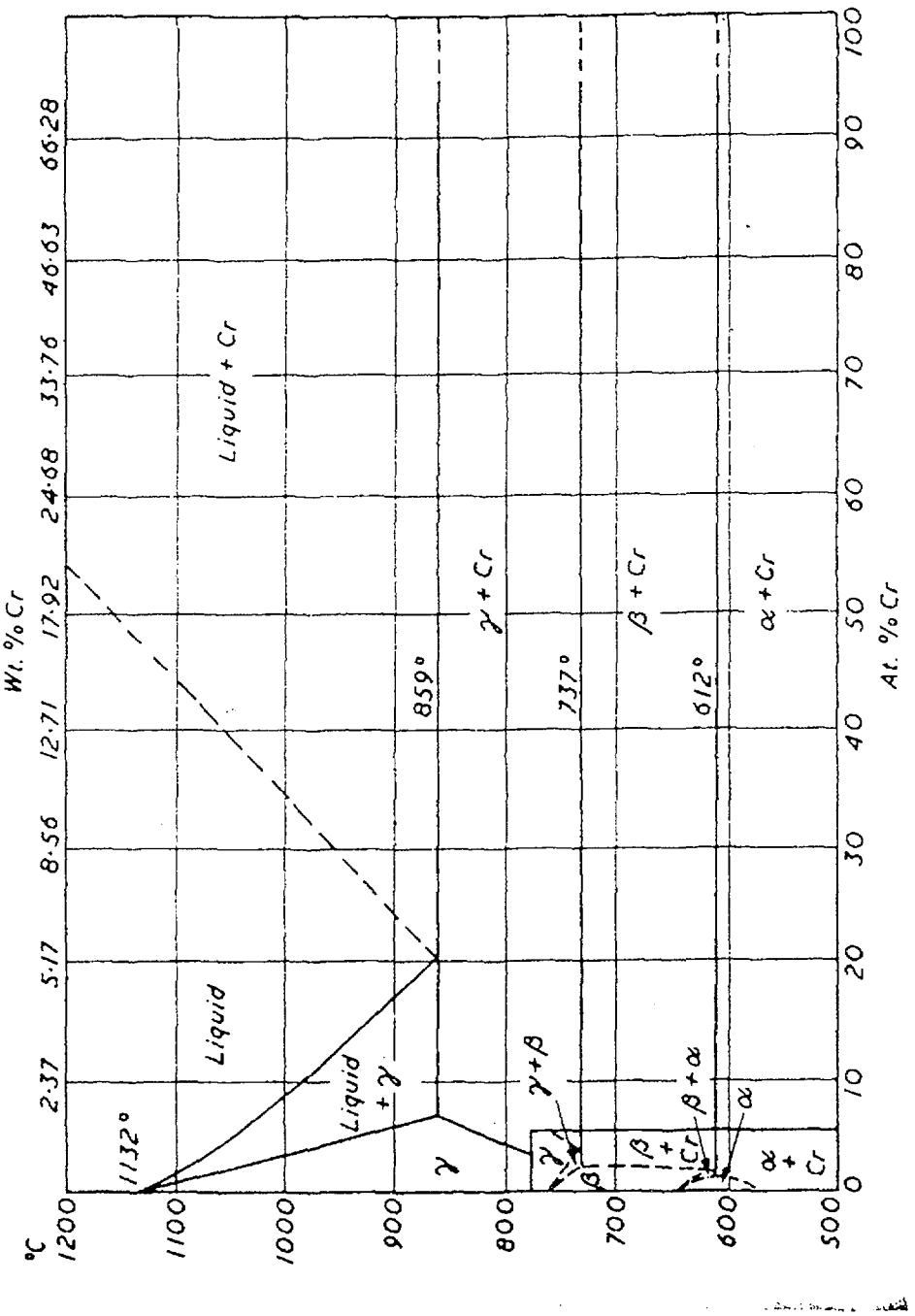

Figure 4. The binary Cr-U phase diagram

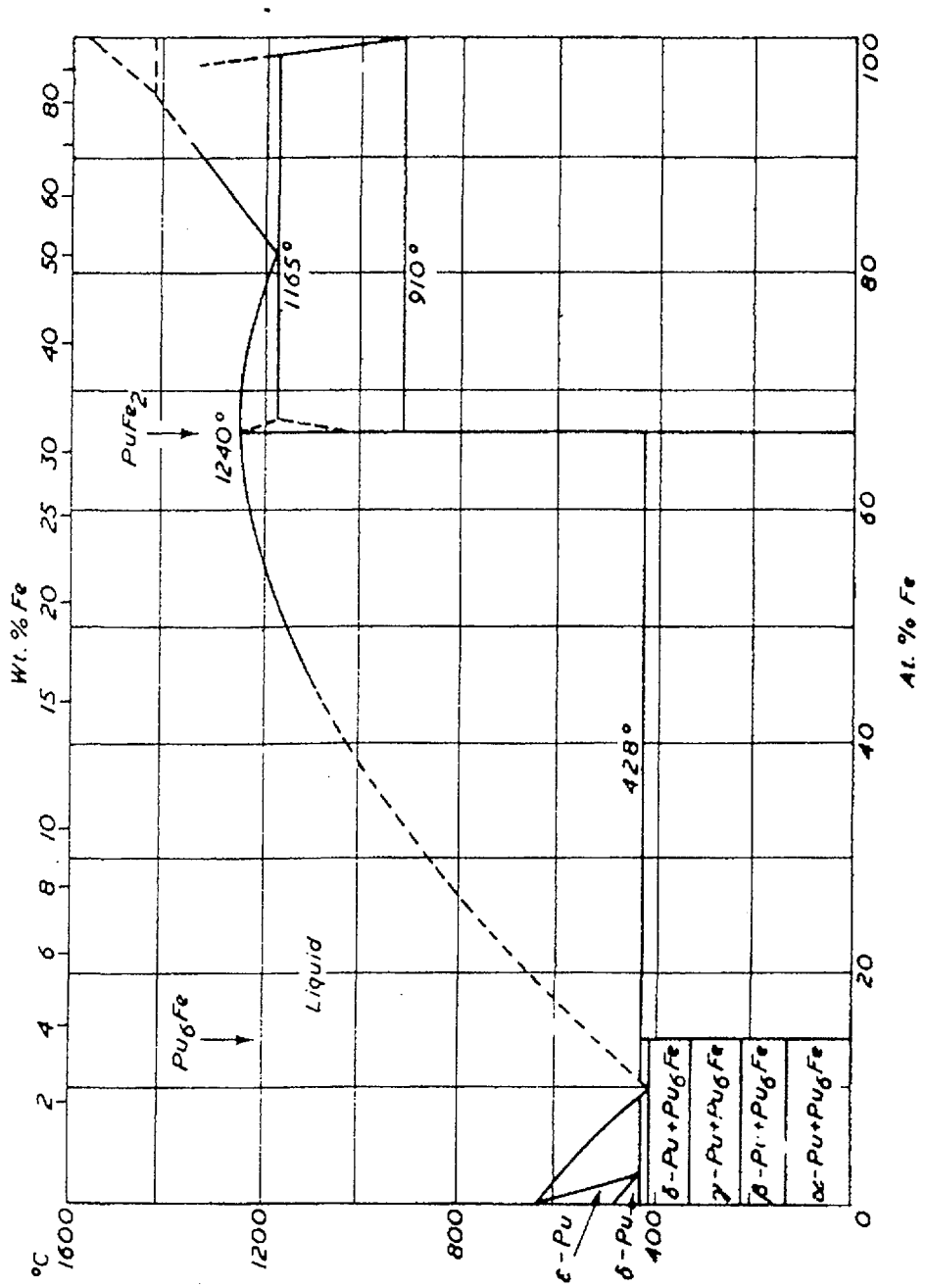

Figure 5. The binary Fe-Pu phase diagram

5. EXPERIMENT REQUIREMENTS

5.1 Homogenization

The fuel shall be homogenized at 900 °C for 4 days. After homogenization, the metallographic examination of specimen will be performed using EDX or EPA (electron probe analyzer).

5.2 Oxidation

The surfaces of the fuel alloys and HT9 rod shall be polished through 0.1 μm alumina to remove the oxidation layer. During annealing and quenching, the provision will be provided to keep the specimen from free of oxidation.

5.3 Dimension Measurement

Before assembling the specimen, the thickness of each specimen shall be measured of the accuracy of ± 0.1 mm. Each specimen should be parallel in thickness. The diameter of HT9 specimen should be larger than the fuel specimen to compare the reaction layer after experiment.

5.4 Temperature Control

The temperature gradient over the length of stacked specimens should be less than 1 °C and the temperature controlled to ± 4 °C in steady-state annealing.

5.5 Duration Time

To determine the duration time of the experiment, the depth of maximum reaction layer is pre-estimated using the empirical correlation of reaction rate between metallic fuel and stainless steels.

$$R = \exp\left(11.646 - \frac{15665}{T}\right) \qquad (1)$$

where R is reaction rate in μm/sec and T is temperature in Kelvin. Fig.6 shows the calculated depth of reaction layer using equation (1).

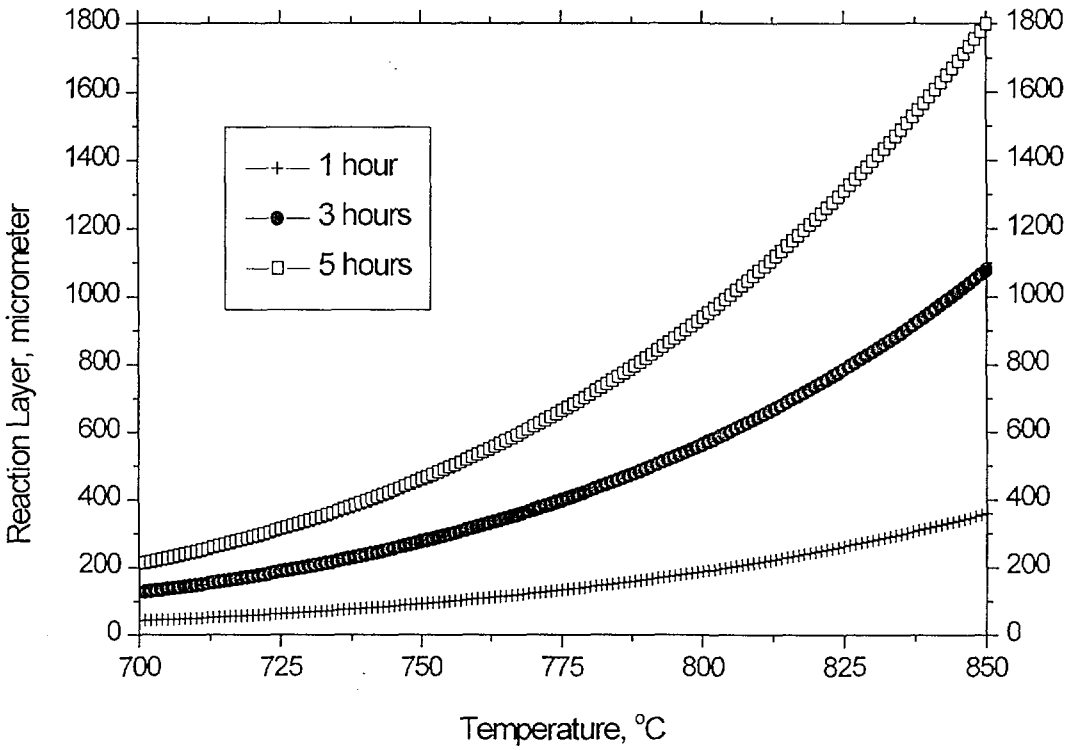

Fig.6 Calculated depth of reaction layer with respect to duration time.

The 3-hour test at 800 °C is expected 2.2 mm of reaction layer on HT9 specimen. It means 44% wastage of HT9 if 5 mm thick slice is used. In addition to this point, the equation (1) is derived based on 1-hour test, so that 1-hour test is preferable.

5.6 Pressure

During experiment, liquefaction of the reaction layer may result in collapse of the specimen thickness. Therefore compressive pressure should be applied continuously at both side of specimen assembly during annealing.

6. TEST PROCEDURES

A series of ex-reactor tests are performed to assess and study the potential problems between U-Zr fuel and HT9 cladding. Diffusion couples of U-Zr with various contents of Zr and HT9 steel are annealed at temperatures ranging from 720 ℃ to 760 ℃ for 100～500 hours in an argon atmosphere, with the longer times generally associated with the lower temperatures. Optical microscopy and SEM examination shall be used to determine whether or not melting had occurred.

6.1 Alloy and cladding preparation

U-Zr fuel alloys with various contents of Zr shall be prepared by "metallic fuel fabrication technology development project". The diameter of fuel slug shall be fabricated according to the KALIMER fuel design as shown in Appendix C. The HT9 cladding steel for the experiment shall be provided by "metallic fuel design development project".

For HT9 cladding material, nominal composition of HT9 cladding is shown in Table 1.

Table 1. Nominal composition of HT9 in weight percent

C	Si	Mn	Cr	Ni	Mo	W	V
0.20	0.4	0.55	11.5	0.5	0.5	1.0	0.3

6.2 Procedures

The disks of various U-Zr alloys and the HT9 cladding steel shall be cut and metallographically polished. This procedure is employed to ensure that the surfaces are free from an oxide layer. During polishing, thickness measurements shall be made to ensure that both faces of the disks are flat and parallel to each other. Fuel and cladding samples are alternatively stacked, like "sandwiches", in columns of up to 3 samples. Experience by ANL has shown that the surface condition in the diffusion-couple experiments is very important. Clean surfaces of a good contact yield lower melting temperatures. Conversely, dirty surfaces that present barriers to

diffusion and will significantly increase the time required for formation of liquid phases at the fuel/clad interface. Therefore, poor contact does not give a proper 'onset-of-melting' temperature. Immediately after polishing, a test column shall be assembled in an "Atmosbag" by stacking the sample into a fixture. Clean surfaces prior to assembly shall be prepared by polishing on a small pad with diamond paste and cleaning with alcohol inside the "Atmosbag". The specimens shall be clamped together in a jig that consisted of two end plates, as shown in Figure 7. The base of this fixture shall be a Kovar alloy (Fe-29Ni-17Co-0.3Mn-0.2Si, w/o) disk with three tapped holes in which threaded Kovar rods are fastened. The threads of these rods shall be upset on the underside of the disk so that the rods are locked in place. This assembly shall be held by a brass pot-chuck while specimens are stacked. A second Kovar alloy disk shall be aligned with the threaded rods and placed atop the stack. Stainless steel nuts shall be then tightened on the threaded rods to put a compressive stress on the test column. A thermal expansion difference between the Kovar alloy rods and the test column ensured axial compressive loading of the samples during annealing.

The assembled couples shall be placed in a quartz tube that is fabricated by "metallic fuel fabrication technology development project". To reduce oxidation of the samples, the fixtured test column shall be quickly inserted into a quartz tube. Each quartz tube shall be flushed several times with argon, evacuated to vacuum, and sealed to form a capsule. The heat-up rate shall be typically about 10℃/sec, hold times at temperature are described in table 2 and table 3. Results of prior calibration tests have established the accuracy of the temperature measurements to be within ± 4℃.

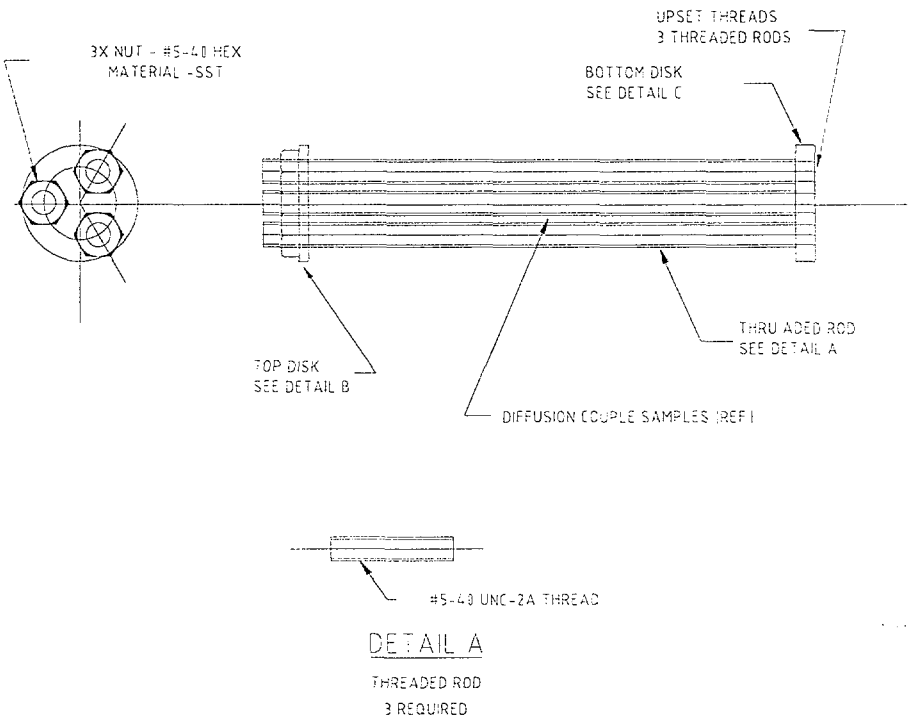

Figure 7. Kovar fixture : assembly and details

The heat-up rate shall be typically about 10℃/sec, hold times at temperature are described in table 2 and table 3. Results of prior calibration tests have established the accuracy of the temperature measurements to be within ± 4℃.

The selected temperature ranges for these experiments shall be 740 ℃ to 760 ℃ for EM1 ~ EM3, which are cover the eutectic temperature of ~740 ℃ for the U-Zr system. For EM4 experiment, the selected temperature and hold time are 720 ℃ and 500 hours, as shown in table 3. For EM1-EM3 experiments, the experimental conditions are given in table 2.

Table 2. Hold times at temperature for EM1-EM3 specimens

Procedure	Specimen Alloy ID	Test Temperature (℃)	Test Duration (Hr)	Remarks
1	EM1	740	100	Check melt and do metallurgical analysis
2	EM2	750	100	
3	EM3	760	100	

After the test, the specimen shall be metallographically examined to evaluate eutectic formation and fuel/HT9 interaction. Before examination, the specimen shall be mounted. The specimen shall be ground and then polished. From the photomicrographs, the thickness of the thinnest remaining cladding shall be determined based on metallographic length standards. The difference between the as-built cladding thickness and the remaining thickness shall be defined as the depth of the cladding penetration. Some cases, the couples shall be analyzed using an optical microscope, or scanning electron microscopy (SEM).

Table 3. Hold times at temperature for EM4 specimen

Procedure Specimen	Alloy ID	Temperature (℃)	Duration (Hr)	Remarks
1	EM4	720	500	Perform metallurgical analysis

7. TEST RESULTS AND COMPARATIVE ACCEPTANCE CRITERIA

The post-test analysis of the diffusion couples includes : metallographic examinations, scanning electron microscopy, and scanning Auger microscopy. Interaction between fuel and cladding under heating condition can result in the formation of phases that degrade the performance of the cladding, and as a result, diffusion couple techniques have been employed to study the relative inter-diffusion behavior of fuel and cladding components. To compare the inter-diffusion behaviors in HT9 cladding with the behaviors reported in U-10Zr fuel versus HT9 cladding steel investigations, comparative criteria are described.

The following sections describe the relevant test results that are needed for this experiment as a design data base.

7.1 Documentation and experimental results

The experiment shall be carried out according to written procedures prepared by the engineer of metallic fuel fabrication technology development and approved for use by the engineer of metallic fuel design development. All experimental results shall be documented in a test report that shall be issued to metallic fuel design development for approval. The final approved test report shall then be issued at revision 0 for use.

7.2 Comparative acceptance criteria

7.2.1 Eutectic formation and threshold temperature

Optical microscopy shall be used to decide whether or not melting had occurred for these samples. Indications shall be given as to whether or not liquid phases formed under the condition of each test.

When zirconium contents are varied to U-fuel, fuel/cladding compatibility and the solidus temperature of the alloy are significantly changed. If the temperature is raised above the eutectic temperature of the alloy, the fuel can form a mixture of liquid and solid phases that may promote further cladding interaction.

The following characteristics are to be observed during the experiment :

- optical observation to form liquid phases.

Subsequent to eutectic formation, additional work shall be performed in which time is included as a variable. The following characteristic is to be observed during the experiment :

- threshold temperatures of each alloy to form combined liquid and solid phase in interface area of fuel/cladding.

7.2.2 Cladding penetration and metallurgical changes in the cladding

Metallograpy shall be conducted on every experimental specimen to search for evidence of liquid phase formation and to measure the extent of penetration for cladding interaction and the formation of a liquid phase to together with the solid. For conservatism, only the maximum penetration shall be measured and reported after the completion of each experiment. Selected samples shall be analyzed by electron microprobe analysis (EMP) and scanning electron microscopy (SEM) to determine the phases and constituents present in the fuel and cladding after FCCI (fuel/cladding chemical interaction) melting and to provide insight into the FCCI mechanism.

- The maximum depths of cladding penetration from the 4 tests shall be measured and compared with previous data as described in Appendix B.
- The variation of cladding penetration rates with test temperature, and time at test temperature
- Diffusion layer on the fuel side.

8. REFERENCES

1. A.S Cohen, H. Tsai and L.A. Neimark, "Fuel/cladding compatibility in U-19Pu-10Zr/ Ht9-clad fuel at elevated temleratures", Journal of Materials 204(1993)244-251.
2. C. Sari and C. T. Walker, "Interaction of U-Pu-Zr alloys containing minor actinides and rare earths with stainless steel", Journal of Nuclear Materials 208 (1994) 201-210.
3. D.C. Crawford, C.E. Lahma, H. Tsai, and R.G. Pahla, "Performance of U-Pu-Zr fuel cast into zitconium molds, Journal of Nuclear Materials, 200 (1993) 157-164.
4. D.D.Keiser, Jr. and M.A.Dayananda, "Interdiffusion between U-Zr fuel and selected Fe-Ni-Cr alloys", Journal of Nuclear Materials 200 (1993) 229-243.
5. G.L. Horfman, A. G. Hins, D.L. Porter, L. Leibowitz, and E. L. Wood, " Chemical Interaction of Metallic Fuel with Austenitic and Ferritic Stainless Steel Cladding", Proceedings of Reliable Fuels for Liquid Metal Reactors, Tucson Arizona, Sep. 7-11, 1986.
6. G.L. Horfman and L.C. Walters, "Metallic Fast Reactor Fuels" Materials Science and Technology, chapter 1, Nuclear Materials, Part 1,VCH Verlagsgesellschaft mbH, 1994.
7. H. Tsai. "Behavior of Low-burnup Metallic fuels for the Integral Fast reactor at elevated temperatures in Ex-reactor tests", FR'91 Proceedings Vol. III, International Conf. On Fast Reactors and Related fuel Cycles, October 28-Nov.1 Kyoto, P1.18-5, 1991.
8. L. Leibowitz, R.A. Blomquist and A.D. Pelton, "Thermodynamics of the Uranium-Zirconium system", Journal of Nuclear Materials 167 (1989) 76-81.
9. P.C. Tortorici and M.A Dayananda, "Interdiffusion of cerium in Fe-base alloys with Ni or Cr", Journal of Nuclear Materials 204 (1993) 165-172.
10. R.G. Pahl, C.E. Lahm and S.L. Hayes, "Performance of HT9 clad metallic fuel at high temperature", Journal of Nuclear Materials 204 (1993) 141-147.

APPENDIX A . Fuel-Cladding Chemical Interaction

Fuel-cladding chemical interaction (FCCI) in an all-metallic fuel element is essentially a complex multicomponent diffusion problem. Characterization of fuel-cladding interdiffusion is exceedingly difficult because of the number of alloy components involved. With stainless steel cladding, even in the most simple fuel alloy such as U-Fs and U-Zr, at least five major constituents participate in the diffusion process. In addition, minor alloy component such as C, N and O, as well as fission products - particularly at higher burnup - appear to play an important role. The potential problem of interdiffusion of fuel and cladding components is essentially two-fold: weakening of cladding mechanical properties and formation of relatively low melting point compositions in the fuel. In an attempt to assess the severity of these two deleterious effects prior to irradiation testing of specific fuel elements, one customarily performs diffusion couple experiments in the laboratory.

During the 1960's ANL tested a large number of fuel-cladding combinations with this diffusion method. It was concluded that the 300 series of austenitic stainless steel cladding has an acceptable degree of cladding attack for U-Fs fuel. However, the addition of Pu increased the rate of attack, and more importantly, decreased the temperature at which melting was observed in the diffusion zone. As shown in Fig. A1 and Table A1 (Zegler and Walters, 1967), a marked improvement in both diffusion rates and minimum melting temperature was obtained through the addition of at least 10 wt.% Zr in the fuel alloys. Whereas Ti was also considered as a fuel alloy addition, but proved to be ineffective. This discovery forms the basis for the selection of 10 wt.% Zr alloys for the present IFR fuels.

Table A1. Melting temperatures from diffusion couple data after 300-700 hours at temperature.

Cladding/Fuel Couples	T_m in °C			
	304	316	HT-9	D-9
U-8 Pu-10 Zr	> 760	790	<750	740
U-19 Pu-10 Zr	> 780	790	>780	>730
U-26 Pu-10 Zr	-	< 775	650	650
U-15 Pu-10 Zr	> 800	> 800	>800	>800

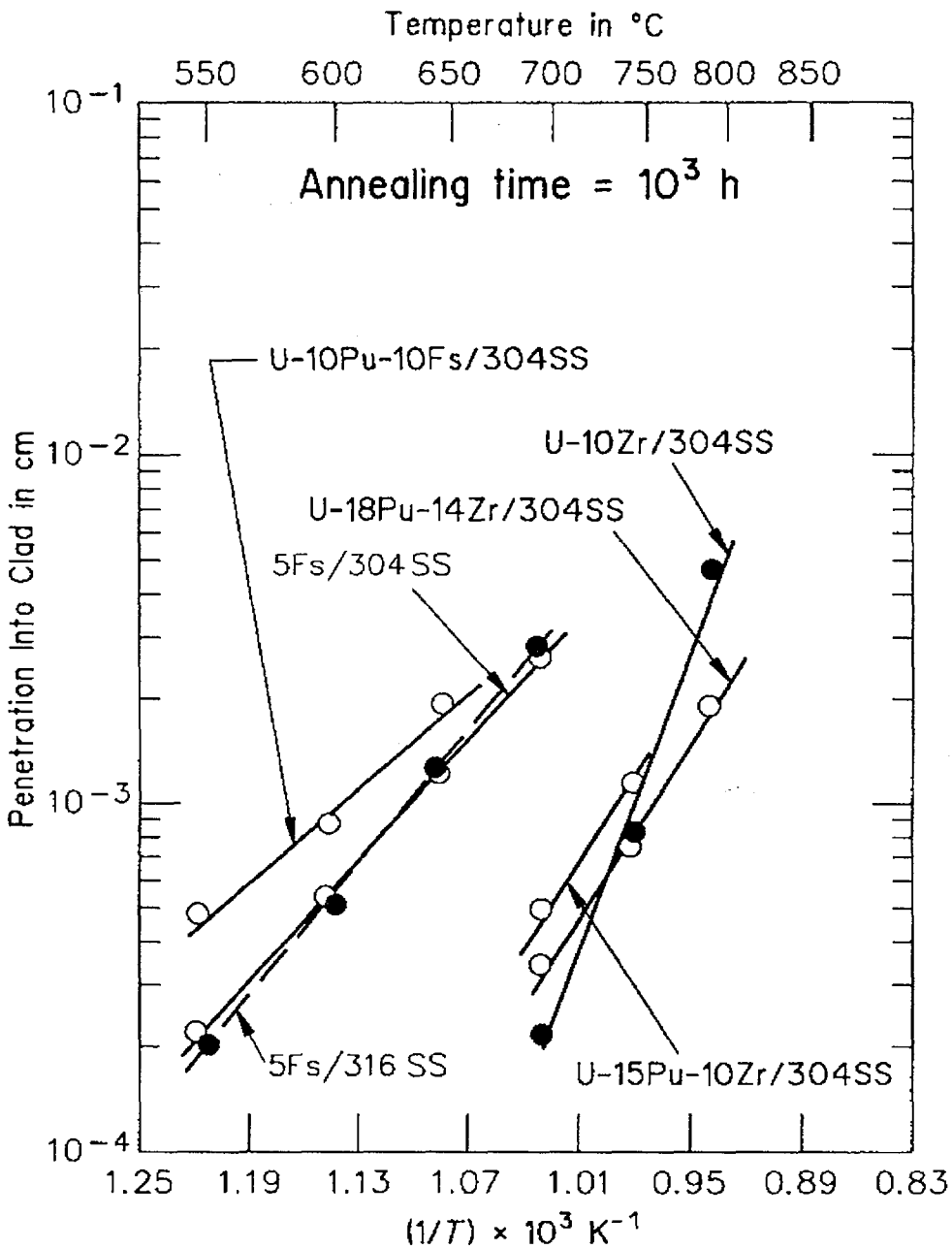

Figure A1. Depth of interaction layer in cladding for various fuel-cladding diffusion couples (Zegler and Walters, 1967).

Considerable variability in austenitic cladding attack was observed with U-18Pu-14 Zr; for example, type 310 showed a depth of 30-44μ m after 5000 hours at 750℃(similar to type 304), while type 309 showed less the 8μ m. However, in none of these combinations did melting occur after 5000 hours at 800℃ (Zegler, 1967). It was concluded that the variability in cladding attack was due to the formation of thin layers of oxygen-stabilized Zr, which formed at the original fuel-cladding interface. These layers act as diffusion barriers, and the extent of their formation would depend on the oxygen activity in the stainless steel, which could vary from type to type. It is of interest to note the limited test result then obtained on ferritic type 440 stainless steel because of the current use of ferritic-martensitic cladding. Diffusion tests with U-10 Pu-14 Zr and this ferritic steel showed molten phase formation at 750℃ after only five days. This inferior behavior, compared to austenitic steels, removed the ferritic steels from further consideration in the 1960's.

These results and earlier data reported by Kittel (1949) on diffusion experiments with uranium (see Fig. B1) also lead the researchers to conclude that Ni played an important role in fuel-cladding interdiffusion. These findings and conclusions are relevant to the newly developed low-swelling cladding materials used for the IFR fuel elements.

The austenitic cladding D-9 contains Ti, which forms extremely stable with interstitial elements in the steel, rendering these elements unavailable for the possible formation of a Zr-compound diffusion barrier. On the other hand the martensitic steel HT-9 contains very little Ni and might be expected to behave like the aforementioned type 440 stainless steel.

In order to assess specifically the propensity for molten phase formation, diffusion experiments were performed with the current IFR fuel-cladding combinations. Series 300 stainless steel were included, as well as fuel sample from an archive fuel element that was fabricated in 1967 for comparison with the previous experiments. The results of these experiments are summarized in Table A1 below. They are "consistent" with 1960's data: there is considerable scatter in both sets of data in regard to various fuel/cladding types, but in the same wide range of results.

The result of this sort of testing have shown many indications as to the influence of the formation of a surface layer of zirconium containing 20-30 at.% of interstitial elements (O, N, C), as was found in the 1960's studies (oxygen was thought to play a dominant role). The interstitial element found in greatest at

abundance in the interface zirconium layers found in the recent work (Hofman et al., 1986) was nitrogen. Moreover, it seemed that thicker layers were formed in couples where the nitrogen content of the cladding alloy was greatest. It was, therefore, speculated that the enhanced compatibility of the 316 couples, compared to the D9 and HT9 alloys, was due to the 600ppm N contents vs. 40-50ppm in the HT9 and D9 alloys. The increased carbon content was apparently not effective in enhancing HT9 compatibility compared to the 316 and D9 austenitic alloys, perhaps due to carbide stability at T >700℃.

Another indication of the nitrogen effect on inter-diffusion is that none of the diffusion couples containing the 1967 archive fuel showed any evidence of melting at the highest temperature of 810℃, and that they had formed much thicker Zr layers at the fuel-cladding interfaces. While the carbon and oxygen content of the various fuel alloys used in the test was similar, the nitrogen content of the 1967 vintage fuels was ~500w/ppm, compared to ~20w/ppm in the current IFR fuel alloys.

Studies were done to show that the presence of small amounts of nitrogen (in a heat treatment atmosphere) can induce the formation of Zr-rich layers on the surface of samples. These layers were then shown to enhance compatibility in subsequent diffusion-couple tests and appear to be effective interdiffusion barriers. The relationship of how the layers form as influenced by test technique, sample preparation, etc., may also explain some of the scatter in the diffusion-couple data.

Metallographic examinations of the various diffusion couples lead to the following general observations (Hofman et al., 1986). A Zr layer containing approximately 20at.% N is first formed at the interface of all fuel-cladding combinations as shown in Fig. A2. This layer is thicker and apparently forms more readily in the case of type 316 stainless steel, which has a rather high dissolved nitrogen concentration. Subsequently, primarily Fe and Ni (in austenitic steels) diffuse into the Zr layer and form two distinct phases that contain some U and Pu as well, indicating that these elements can diffuse through the Zr compounds (see Fig. A2). Finally further diffusion of U and Pu leads to the formation of fuel-cladding component phases equivalent to U_6Fe and UFe_2 on the cladding side of the Zr compound layer. In the case of austenitic steels, the UFe_2 type phase forms a "finger"-like diffusion front, a structure often observed in multi-component diffusion when two of the diffusing species (in the present case Ni and U) diffuse by a

relatively rapid exchange mechanism (Van Loo et al., 1984). The U_6Fe-like phase forms directly behind the "fingers" (see Fig. A3).

The inter-diffusion zone is essentially the same for type 316 and D9 stainless steel, but the rate of formation is much lower for the former, due to the difference in the initially formed Zr-N layer. In the case of basically Ni-free ferritic steel, HT-9, the U_6Fe and UFe_2 type phases form a single zone without the finger-like structure, also shown in the Fig. A2. There exists a eutectic composition between these two phases, the temperature of which depends on the concentration of Pu, Ni and Zr in the phases, as well as U and Fe. However, judging from the data in Table A1 for D9 and HT-9, this temperature appears to lie in the vicinity of U-Fe eutectic of approximately 720℃. Presumably the type 316 stainless steel would have yielded a similar melting temperature had the test run longer, i.e., more U diffusion through the Zr layer should have occurred. As it were, melting in the case of type 316 or 304L occurred near 800℃ and appeared to have started in the fuel side of the diffusion couple. At this temperature the diffusion of Fe and Ni into the fuel, rather than U into the steel, lead to eutectic formation, The eutectic temperature is the Fe-U-Pu-Zr system drops significantly with Pu concentration, which may explain the lower melting temperatures for the 26 wt.% Pu fuel. The melting in this case also started in the fuel side of the diffusion couple.

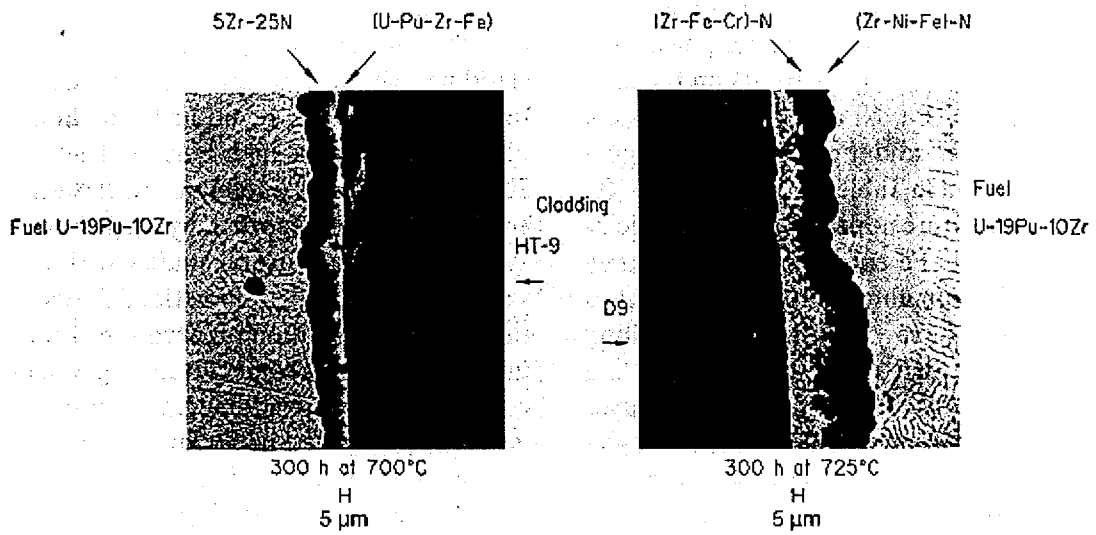

Fig. A2 Layers formed at fuel-cladding diffusion couple interfaces.

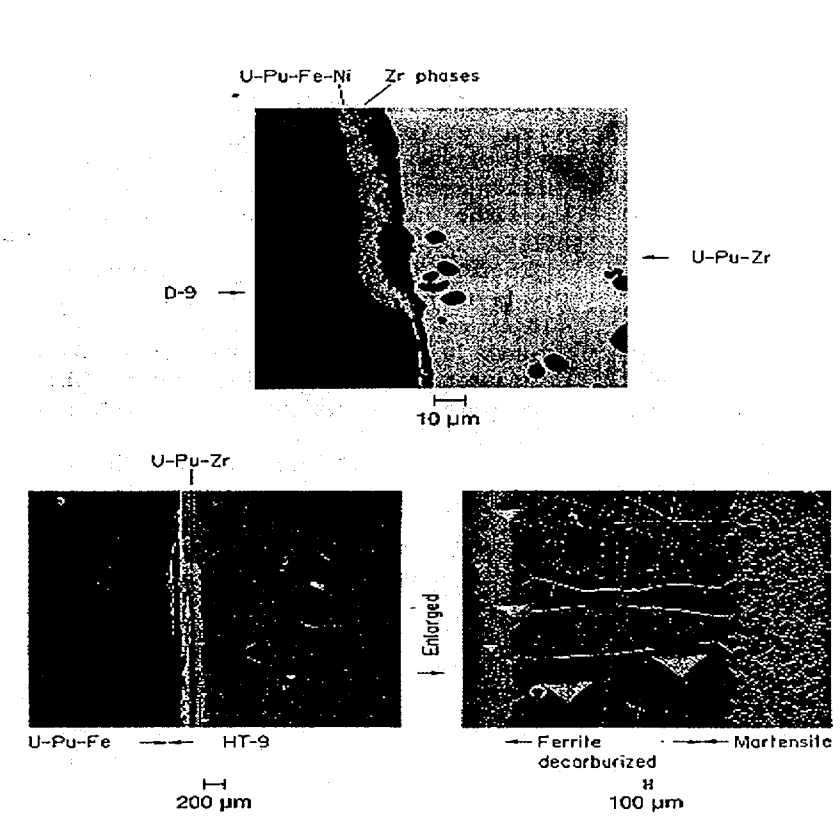

Fig. A3 Interaction layers formed after 300h at 705℃ between D9 steel(upper) and HT-9(lower) and U-19Pu-10Zr fuel(note decarburization in HT-9).

The results obtained with diffusion couples indicate what might occur in reactor during fuel-cladding chemical interaction. However, post-irradiation examinations and annealing experiments with irradiated fuel and cladding show significantly different behavior of FCCI in an actual fuel element. The emphasis in the proceeding discussion of the diffusion couple test has been in the formation of liquid phases, but except during possible transient events, fuel elements operate by design below these melting points. The FCCI during normal operation is thus characterized by solid state interdiffusion. As was suggested earlier, Ni appears to play an important role in FCCI. Preferential diffusion of Ni into the fuel result in a ferritic layer in the cladding of all austenitic steel-fuel combinations. This Ni, as well as some Fe, diffuses into the fuel to a depth several times as large as the Ni-depleted layer in the cladding. The ferritic layer, on the other hand, contains little or no fuel. The inter-diffusion zone in a high-burnup U-5Fs 304L-clad elements (Hofman, 1980) is very similar to those reported by Zegler and Walters (1967) in diffusion studies with the same fuel-cladding combination. A selection of post-irradiation observations listed in Table A2 shows some interesting differences various fuel-cladding combinations. For example, the Ni depletion in type 316 stainless steel is substantially lower than in type 304 for both U-5Fs (Hofman et al., 1976) and U-Pu-Zr (Murphy et al., 1969), where Zegler and Walters found no difference between these two steels in their diffusion studies. Moreover, a difference in radiation-enhanced diffusion of Ni in the two steels does not explain this different behavior. The effect of rare earth fission products on Ni diffusion was considered because these elements are found in the Ni-depleted zone of austenitic steel clad U-Pu-Zr fuel elements up to a concentration of a few percent at 5 at.% Bu (see Fig. A4 and Table A2) and as much as 20% in the high-burnup D9-clad elements as illustrated by Fig. A5 (also reflected in the hardness of the Ni-depleted zone). Rare earth fission products of the lanthanide series migrate readily to the cladding in Pu-containing fuel, but not as easily in U-Zr, which might explain the large difference in layer width between those fuels and D9 cladding. However, there are no rare earth elements found in the Ni-depleted layers in the U-5Fs fuel, yet the difference between type 316 and 304L is of the same order as that U-15Pu-9Zr fuel.

Table A2. Comparison of Ni-depleted zones in various fuel-cladding combinations.

Fuel	Cladding	Ni depleted Zone[a], μm	Bu in at. %	T(BOL) in °C	Ce-Nd in at. %	DPH
U-5Fe	304L	50(10)[b]	10	560	~ 0	230
	316	10(10)[b]	10	560	~ 0	nm[c]
U-15 Pu-9 Zr	304L	140	5	650	Few	280
	316	30	5	650	Few	280
U-9 Pu-10 Zr	D9	100	17	580	~ 20	1050
	316	70	13	580	nm[c]	1000
U-10Zr	D9	20	17	580	nm[c]	nm[c]
U-10Zr	HT-9[a]	100	5	650	3	200
U-19Pu-10 Zr	HT-9	45	12	600		350

[a] Decarburized zone for HT-9 ; [b] extrapolated from Zegler and Walters diffusion couples ; [c] not measured.

There is no satisfactory explanation of this behavior at this points, other than the suggestion that the aforementioned initial Zr-rich layer formation at the fuel-cladding interface of the various fuel-cladding combination sufficiently different, and affected differently enough during irradiation, to alter Ni diffusion from the cladding.

FCCI between austenitic and martensitic steel has both similarities and differences. Because HT-9 contains very little Ni, depletion of this element, which seems to control FCCI in austenitic D9, does not apply to HT-9. However, the ferritic layer in D9 formed by Ni depletion is essentially similar to a ferritic layer in HT-9 that results from decarburization of the original martensite. An example of this is shown in Fig. A6, which was measured after 6 at% burnup at ~620 ℃. Such decarburization and ferrite formation, one recalls, also occured in diffusion couples illustrated in Fig. A3. However, the differences in FCMI between austenitic and martensitic steel may be more significant than are aforementioned similarity. First, the rate of ferrite formation due to decarburization of HT-9 is lower than that due to Ni depletion in D9 at comparable temperatures. Moreover, the diffusion of rare earths into the ferritic layers is quite different for the two steels. Unlike the uniform diffusion in D9, rare earths diffuse only partially along a uniform front, but rather more along grain boundaries in HT-9, as shown also in Fig. A6.

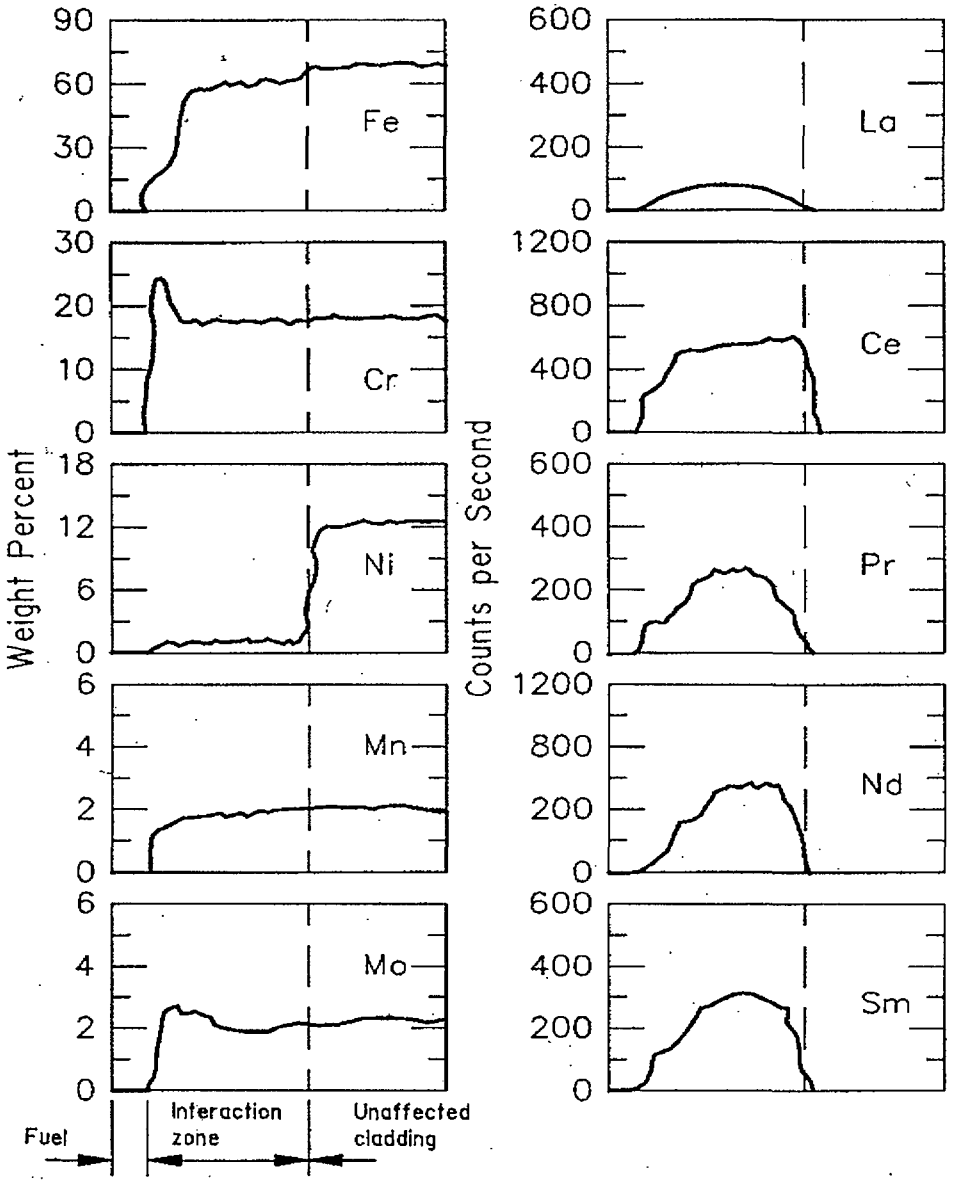

Fig. A4 Electron microprobe scan of interaction zone at U-Pu-Zr type 316 Cladding interface showing Ni depletion and lanthanide penetration (~5 at.% burnup at 640 ℃ cladding temperature)

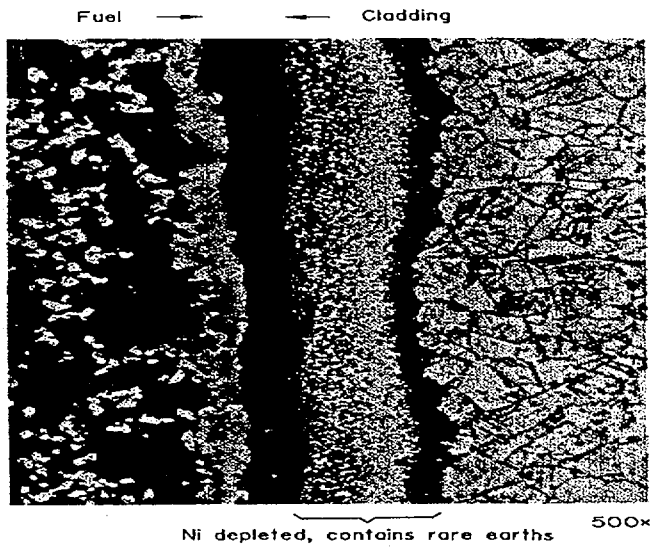

Fig. A5 Micrograph of etched cross-section showing fuel cladding inter-difffusion of U-Pu-Zr and D-9, in pile, after ~ 12 at.% burnup at ~500 ℃.

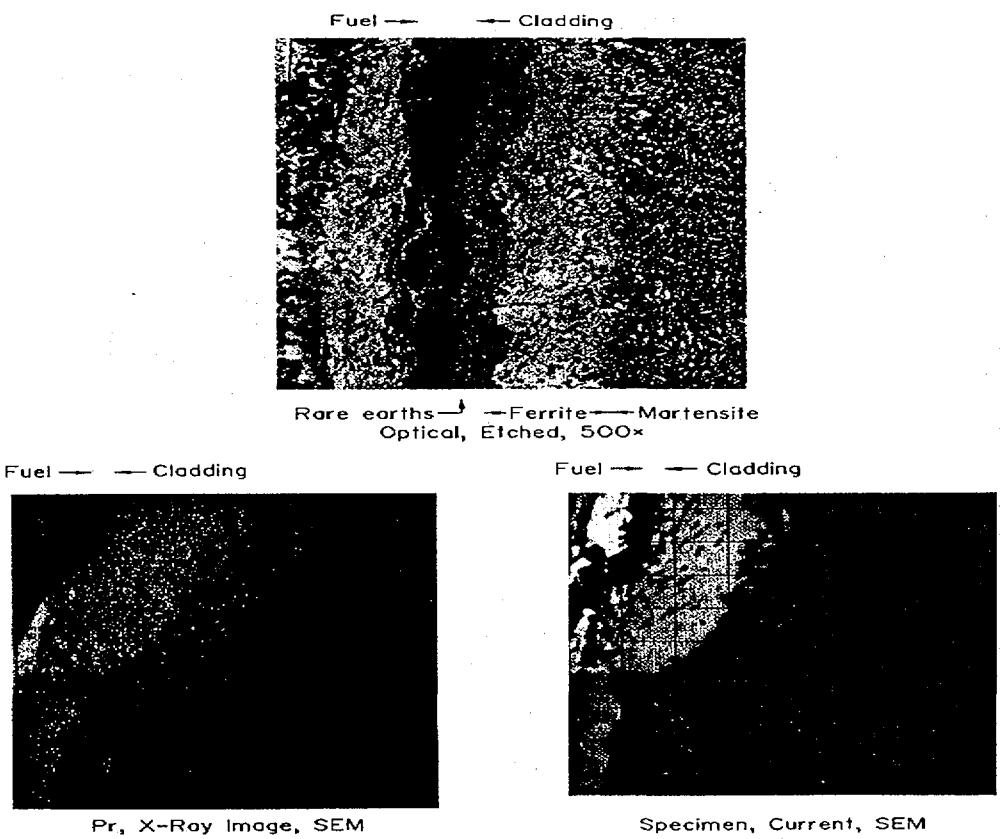

Fig. A6 Fuel-cladding inter-diffusion of U-10Zr and HT-9

Although our understanding of FCCI is not complete at this juncture, it appears that the data allow us to make the following general observations. Prior to accumulation of significant amounts of lanthanide fission products at the fuel-cladding interface, FCCI depends on the particular fuel-cladding combinations; i.e., various degrees of Ni depletion in austenitic cladding and decarburization of martensitic cladding have a solid state diffusion type time and temperature dependence. Lanthanides ultimately control FCCI, but their presence at the internal cladding surface depends not only on burnup but very strongly on their radial migration in the fuel. Although radial lanthanide migration increases with fuel temperature for all fuel alloys, it is most rapid in U-Pu-Zr, less so in U-Zr and least in U-5Fs.

The in situ formation of Zr-N layers in diffusion couples and the reduced Ni depletion found in type 316 stainless steel indicate the feasibility of improving the FCCI. However, the FCCI problem with austenitic cladding might be largely academic, since swelling alone renders these steels unacceptable for use at high burnup. High burnup operation requires a low swelling cladding material such as HT-9, so acceptable FCCI is more important in this steel.

Although melting due to FCCI is not expected at normal fuel element operating conditions, the ex-reactor diffusion test indicate that liquid phase formation needs to be considered if cladding temperatures were to reach the 700℃-800℃ range during transient conditions. In these considered transients, the higher temperatures in this range are reached in events lasting only minutes, while relatively lower temperature events such as loss of coolant combined with a disabled heat rejection system may last many hours. To better characterize liquid phase formation in cladding and fuel at elevated temperatures, sections of various irradiated fuel elements have been heated in an in-cell apparatuses over a range of temperature and time (Tsai et al., 1990). This work has shown no evidence of liquid phase formation below ~725℃ for test durations of up to seven hours, in general agreement with the diffusion experiments discussed before, and has yielded a large body of kinetic data at higher temperature (Tsai et al., 1991). Figure A7 shows an envelope of test results on several fuel-cladding combinations measured as a function of time at 800℃. The broadness of the data range is due to the number of fuel-cladding combinations tested, i.e., 0-26%Pu and type 316, D-9 and HT-9 steels, as well as various burnup levels and irradiation conditions of the tested samples. Further testing is still in progress.

In general, the penetration depths appear to be parabolic functions of time with a power of less than one. The rate of attack is similar for HT-9 and D9, but generally lower for type 316 with all fuel compositions. It is interesting to note that for the parameter range covered thus far in these post-irradiation heating tests, 0 % Pu fuel has shown the highest rate of attack and 26% Pu fuel the lowest, opposite to the trend observed in diffusion couples. Metallographic examination of these post-irradiation samples reveals that the FCCI is similar to that observed in unirradiated diffusion couple tests, with the exception of a pronounced effect of rare-earth fission products in high burnup fuel samples. This experimental program has not advanced to development of a satisfactory fundamental model for the observations. Meanwhile, correlations of cladding penetrations with temperature and time derived from these preliminary test results are used in evaluating transient behavior of metallic fuel elements.

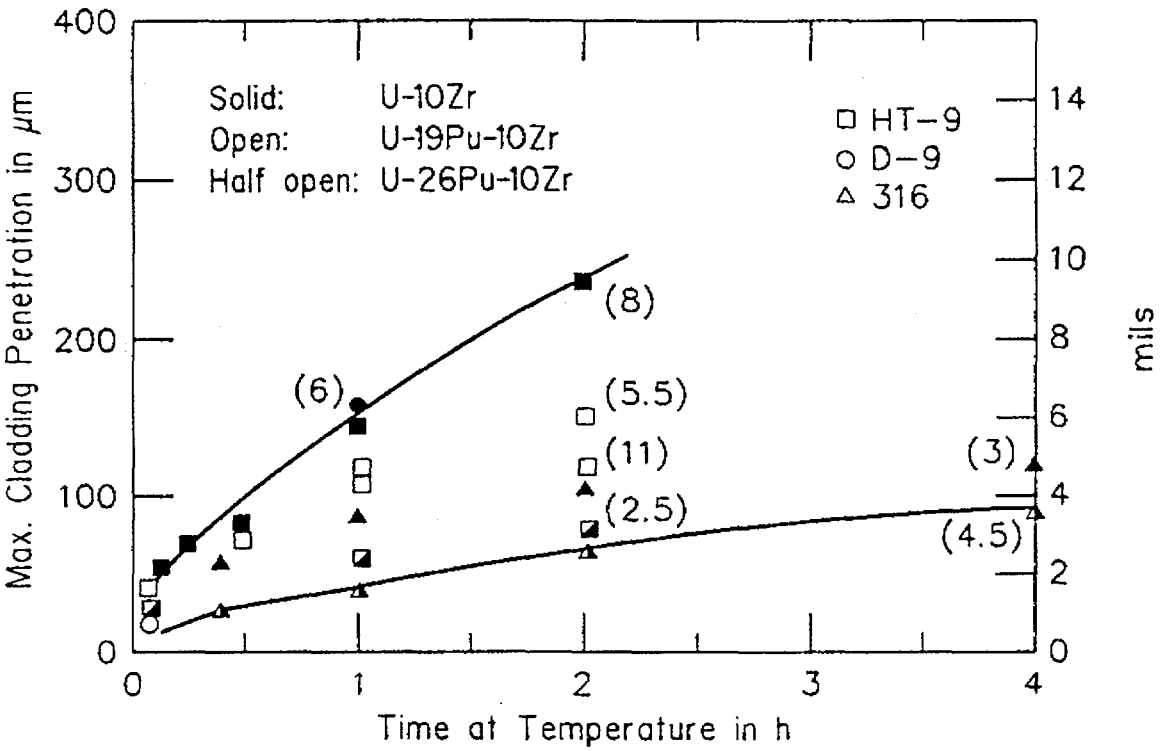

Figure A7. Envelope of fuel-cladding penetration depth as a function of time at 800 ℃ during post-irradiation heating tests (burnup of test samples in blackets) (Tsai, 1991).

APPENDIX B Standard behavior reported in U-10%Zr fuel versus HT9 cladding steel investigations

The results and earlier data reported by Kittel on diffusion experiments with uranium also lead the researchers to conclude that Ni played an important role in fuel-cladding inter-diffusion, as shown in Figure B1. The U_6Fe and Ufe_2 type phases form a single zone without the finger-like structure in martensitic steel HT-9 which contains very little Ni. These exists a eutectic composition between these two phases, the temperature of which depends on the concentration of Pu, Ni and Zr in the phases, as well as U and Fe. Melting temperature from diffusion couple data for U-8Pu-10Zr after 300-700 hours was 740 ℃, this temperature appears to lie in the vicinity of the U-Fe eutectic of approximately 720 ℃[ref1]. The eutectic temperature in the Fe-U-Pu-Zr system drops significantly with Pu concentration, which may explain the lower melting temperatures for the 26 wt% Pu fuel. The melting in this case also started in the fuel side of the diffusion couple. Experimental results[2] for various irradiated fuel elements which were heated in an in-cell apparatus over a range of temperature and time, have shown no evidence of liquid phase formation below ~725 ℃ for test durations of up to seven hours, in general agreement with the diffusion experiments and has yields a large body of kinetic data at higher temperature. An envelope of test results on several fuel-cladding combinations are appeared in Figure B2 and B3, which were measured as a function of time at 800 ℃. Maximum cladding penetrations were ranged from 100 ㎛ to 150 ㎛ for test duration of 1-2 hours.

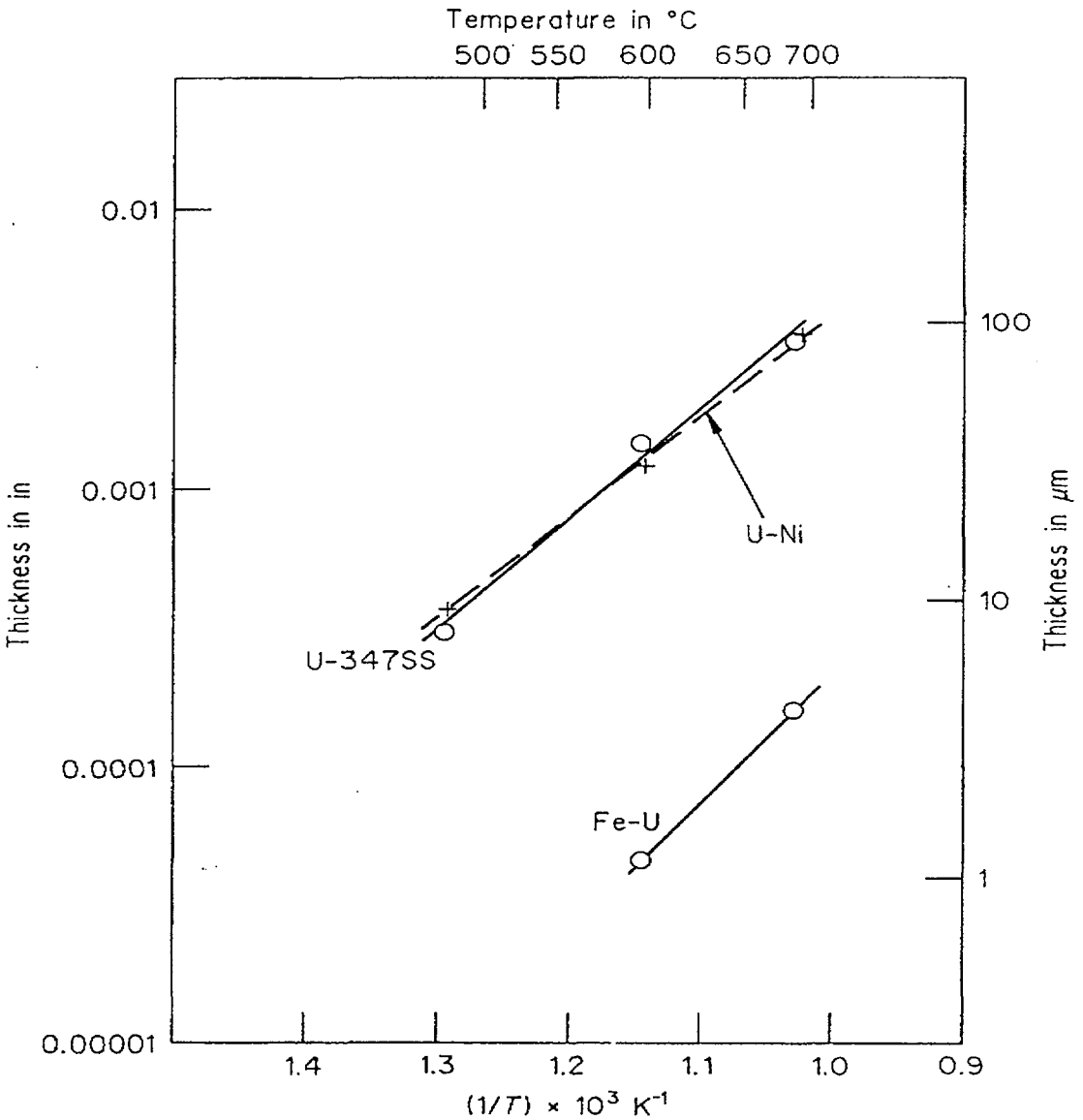

Figure B1. Thickness of interaction layers in diffussion couples after six day anneals.

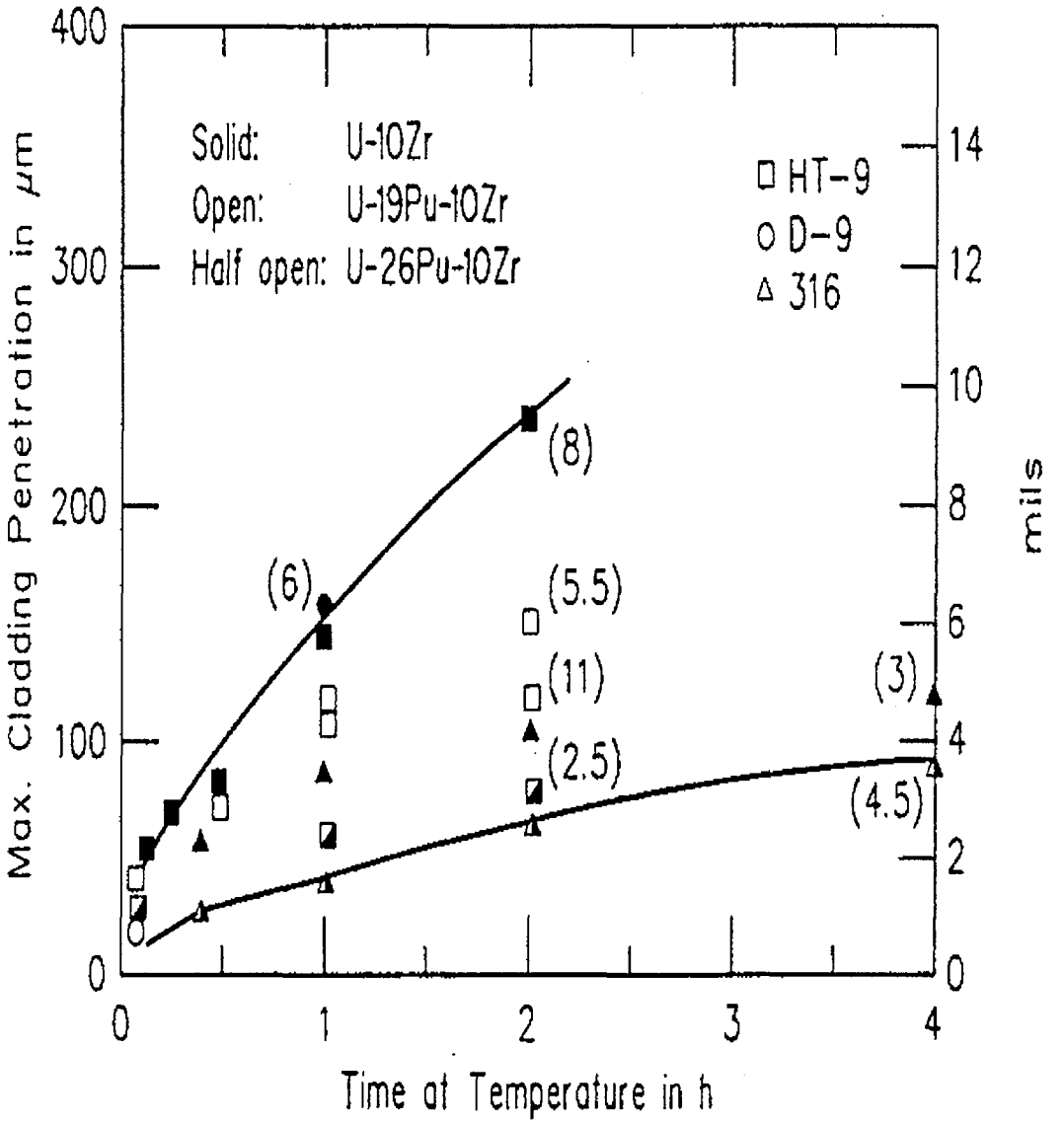

Figure B2. Envelope of fuel-cladding penetration depth as a function of Time at 800℃ during post-irradiation heating tests

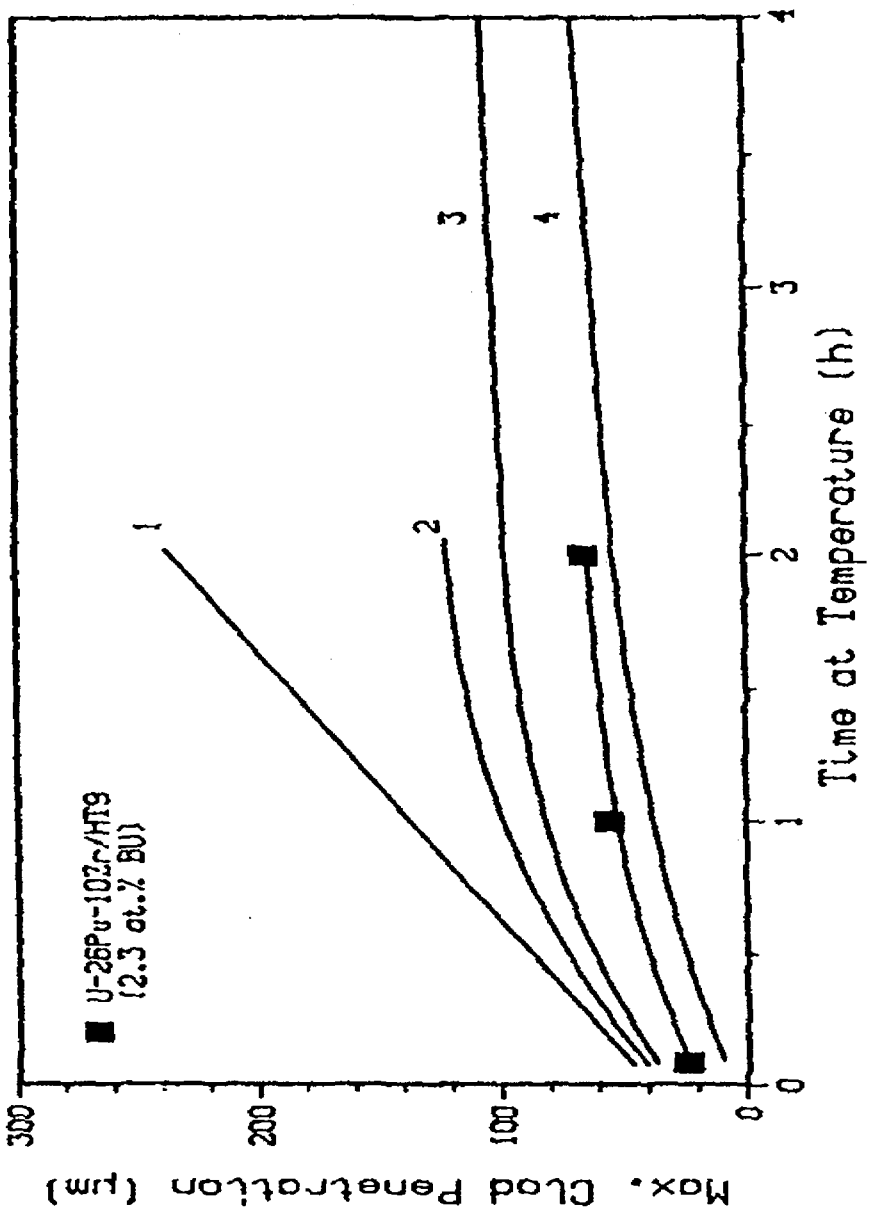

Figure B3. Time dependence of cladding penetration depth at 800℃. Results from tests of other fuel systems are also shown : (1) U-10Zr/HT9 at 8 at.% BU, (2) U-10Zr/D9 at 17 at.% BU, (3) U-10Zr/316SS at 5 at.% BU.

APPENDIX C Preliminary design data of KALIMER fuel rod

Fuel Slug	
- binary	U-10wt%Zr
- ternary	U-Pu-10wt%Zr
Fuel Slug Diameter (mm)	5.46
Fuel Slug Density(g/cm^3)	
- Fabrication	15.58
- TD	17.5
Enrichment of Fuel	
• binary system	
- driver	19.9% U-235
- blanket	depleted U
• ternary	TBD(Pu content)
Smeared Density (%)	75
Fuel Cladding Gap (mm)	0.42
Pin P/D Ratio	1.203
Cladding Material	HT9
Pin Outer Diameter (mm)	7.4
Integrated Gap Between Fuel and Clad (mm)	0.84
Pin Inner Diameter (mm)	6.3
Cladding Thickness (mm)	0.55
Pin Overall Length (mm)	3593.00
• Upper End Plug (mm)	25.40
• Lower End Plug and Shielding (mm)	1117.60
• Upper Gas Plenum Length (mm)	1550.00
- Sodium Filler Height (mm)	250.00
- Net Gas Plenum Length (mm)	1300.00
• Fuel Slug Length (mm)	900.00
Net Plenum Volume (cm^3)	26.42
Fill Gas Pressure (psi)	14.7
Fill Gas	He
Pin Pitch (mm)	8.9
Plenum to Fuel Ratio	2.00
Wire Wrap Diameter (mm)	1.40
Wire Wrap Pitch (mm)	187.2
Bond Material	Na
Gas Tagging System	None

BIBLIOGRAPHIC INFORMATION SHEET			
Performing Org. Report No.	Sponsoring Org. Report No.	Standard Report No.	INIS Subject Code
KAERI/TR-1139/98			

Title/Subtitle : Experimental Specifications for Eutectic Reacton between Metallic Fuel and HT-9

First Author and Department	Hwang, Woan (Metallic Fuel Design Development)

Co-author and Dept. : Nam, Cheol; Lee, Byoung Oon (Metallic Fuel Design Development), Ryu, Woo Seog (Liquid Metal Reactor Materials Characterization)

Pub. Place	Taejon	Pub. Org.	KAERI	Pub. Date	1998. 10
Page	48 p.	Fig. & Tab.	Yes(O) No( )	Size	26 cm
Note					
Classified	Open(O) Outside( ) Class		Report Type	Technical Report	
Sponsoring Org.	MOST		Contract No.		

Abstract (About 300 Words)

The chemical interaction between metallic fuel and cladding is important in designing the fuel pin of the KALIMER. When metal fuel and cladding are contacted, the elements in fuel and cladding are inter-diffuse each other, forming the reaction layers at interface. The reaction layers may cause two important factors in aspects of fuel pin integrity. Firstly, it degrades cladding strength by reducing effective cladding thickness. Secondly, these layers accelerate eutectic reaction at transient conditions.

To evaluate these phenomena, the diffusion couple experiment is planned by using metal fuels with various zirconium contents and HT-9 steel. The U-Zr fuel alloys will be used for the experiment with the different zirconium contents, these are 8, 10 and 12 weight %. This experiment aims to evaluate the effects of zirconium content on the chemical reaction. Furthermore, the reaction rate and threshold temperature of the eutectic melting will be determined as a function of the zirconium content. This document describes the detail experimental specifications for the eutectic reaction such as test setup, test requirements and test procedure.

Subject Keywords (About 10 Words) : eutectic reaction, experimental specification, metallic fuel, FCCI

서 지 정 보 양 식			
수행기관 보고서 번호	위탁기관 보고서 번호	표준 보고서 번호	INIS 주제코드
KAERI/TR-1139/98			

제목/부제 : 금속연료/HT-9강의 공정반응 실험시방서

주저자 및 부서명	황완 (금속핵연료설계개발)

공동저자 및 부서명 : 남 철, 이병운 (금속핵연료설계개발),
류우석 (액체금속로재료평가)

발행지	대전	발행기관	한국원자력연구소	발행일	1998. 10
페이지	48 p.	도표	유(○) 무( )	크기	26 cm
참고사항					
비밀여부	공개(○) 대외비( ) 급 비밀		보고서 종류	기술보고서	
연 구 위 탁 기 관			계약번호		

초록(300단어 내외)

금속연료와 피복관의 화학적 반응은 칼리머 연료봉 설계에 있어서 중요한 고려사항이다. 금속연료와 피복관이 접착하게 되면 다양한 원소의 복잡한 상호확산이 진행되어 반응층이 형성되게 된다. 이렇게 형성된 확산영역은 연료봉 건전성 측면에서 두가지 중요한 문제점을 야기한다. 첫 번째는 피복관의 기계적 강도가 약해지는 점이고, 두 번째는 연료와 피복관의 경계면에서 융점이 낮아지는 공융현상이 나타난다.

이러한 영향을 평가하기 위해서, 확산쌍 실험이 수행될 예정이다. 이 실험에서 사용될 확산쌍은 HT-9강과 U-Zr 금속연료이며 U-Zr 합금의 지르코늄 함량은 8%, 10%, 12%로 각기 다르게 한다. 이 실험의 주 목적은 HT-9 피복관을 가진 U-Zr 금속연료의 지르코늄 허용량을 평가하기 위한 실험 데이터를 생산하는 것이다. 또한 각 시편의 확산쌍 경계면에서 공융현상이 일어나는 문턱 온도와 반응속도를 결정한다. 따라서 본 보고서는 이러한 실험을 수행하기 위한 실험시방 항목들, 즉, 실험설정, 실험요건, 실험절차 등에 대해 기술한다.

주제명 키워드 (10단어 내외): 공정반응, 실험시방서, 금속연료, HT-9, FCCI